Journal of Thermal Analysis and Calorimetry
https://doi.org/10.1007/s10973-020-09328-0

Structure and Raman spectra of binary barium phosphate glasses

Branislav Hruška[1] · Rajesh Dagupati[1] · Mária Chromčíková[2,3] · Aleksandra Nowicka[1] · Jaroslava Michálková[1] · Jacob A. Peterson[1] · Marek Liška[2,3] · Francisco Munoz[4]

Received: 7 November 2019 / Accepted: 11 January 2020

Abstract

The structure of xBaO·(1 − x) P_2O_5 (x = 0.30, 0.35, 0.40, 0.45, and 0.50) glasses was studied by Raman spectroscopy and thermodynamic model Shakhmatkin and Vedishcheva (SVTDM). The seven system components (defined as stable crystalline phases of the BaO–P_2O_5 binary phase diagram) were considered in the SVTDM: BaO, P_2O_5, 4BaO·P_2O_5 (B4P), 3BaO·P_2O_5 (B3P), 2BaO·P_2O_5 (B2P), BaO·P_2O_5 (BP), and BaO·2 P_2O_5 (BP2). Only the equilibrium molar abundances of BP and BP2 were non-negligible in all studied glass compositions. Therefore, in the next step, multivariate curve analysis (MCR) of the baseline—subtracted, thermally—corrected experimental Raman spectra, was performed for two components (BP2 and BP). MCR resulted in the Raman spectra (loadings) and relative abundances (scores) of each considered component. The MCR method reproduced 98.93% of the spectral data variance. Then, the decomposition of Malfait was used. The perfect fit between the MCR loadings and the partial Raman spectra of BP2 and BP, obtained by Malfait's decomposition, was found, confirming the validity of thermodynamic model.

Keywords BaO–P_2O_5 · Thermodynamic model · Raman spectra · Phosphate glass · MCR

Introduction

In comparison with silicate or borate glasses, phosphate glasses possess interesting functional properties, mainly the higher refractive indexes, the lower melting temperature, and thermal expansion coefficients, and high transparency in the ultraviolet range [1, 2]. On the other hand, phosphate glasses have poor chemical durability. The chemical durability and additional properties of phosphate glasses can be improved by the addition of various metal ions into the phosphate network [3, 4]. Due to this compositional variability, phosphate glasses can be used for metal sealing applications, photonics, radioactive waste vitrification, medical applications, etc. [5–7].

The SVTDM enables the interpretation of the relationships between the composition, structure, and properties [8–15]. The validity of the model has to be confirmed by the comparison of its results with the available structural data [13–16]. In our previous work [16–19], we showed that the statistical analysis of the compositional and temperature series of Raman spectra validated the SVTDM thermodynamic model for the Na_2O–B_2O_3, CaO–P_2O_5, and ZnO–P_2O_5 binary glass systems. The main aim of this work is to produce a thermodynamic model to describe the structure for the BaO–P_2O_5 binary glasses.

Method

Thermodynamic model of Shakhmatkin and Vedishcheva

SVTDM was successfully applied to the study of silicate glasses [8–16]. This model uses the assumption that glasses and melts are ideal solutions formed from products of equilibrium chemical reactions between the simple chemical

✉ Branislav Hruška
branislav.hruska@tnuni.sk

[1] FunGlass, Alexander Dubček University of Trenčín, Študentská 2, 911 50 Trenčín, Slovakia

[2] VILA – Joined Glass Centre of the IIC SAS, TnUAD, FChPT STU, Študentská 2, 911 50 Trenčín, Slovakia

[3] Institute of Inorganic Chemistry of Slovak Academy of Sciences, Dúbravská cesta 9, 845 36 Bratislava, Slovakia

[4] Institute of Ceramics and Glass (CSIC), Kelsen 5, 28049 Madrid, Spain

Published online: 27 January 2020

entities (oxides, halogenides, etc.) and from the original un-reacted entities. The model only uses the molar Gibbs energies of pure crystalline compounds and the analytical composition of the system that is being considered. The equilibrium molar amount of each of the systems species is obtained by minimization of the system's Gibbs energy constrained by the overall system composition [20]. SVTDM can be applied to most multicomponent glasses using crystalline state data. The contemporary databases of thermodynamic properties (e.g., FACT database [21, 22]) enable the routine construction of the SVTDM for various multicomponent systems.

Malfait's decomposition of Raman spectra

The basic assumption of Malfait's method [23–25] is that the Raman spectra can be expressed as the sum of partial Raman spectra (PRS) of individual system components multiplied by its equilibrium amount. The linear vector space with the dimensionality given by the number of species with different PRS that independently vary their abundance is spanned by the Raman spectra obtained for series of glasses with different compositions. Arbitrary scaling is used when recording each experimental spectrum. The number of independent components can be determined by principal component analysis (PCA) of the set of experimental Raman spectra [26, 27]. It is worth noting that the field of thermal analysis finds the PCA to be very advantageous [28].

Multivariate curve resolution

The set of experimental Raman spectra can be decomposed by the multivariate curve resolution (MCR) method [29, 30] on the spectra of quasi-pure components (loadings) and relative abundances of these components (scores). The comparison of MCR with PRS of Malfait's decomposition based on the SVTDM can be used for confirmation/validation of SVTDM.

Experimental

The compositional series of binary barium phosphate glasses containing 30, 35, 40, 45, and 50 mol% of BaO, abbreviated as 70P30B, 65P35B, 60P40B, 55P45B, and 50P50B were studied. The glass batches were prepared from analytical grade ammonium dihydrogen phosphate ($NH_4H_2PO_4$) and barium carbonate ($BaCO_3$). Stoichiometric quantities of $BaCO_3$ and $NH_4H_2PO_4$ were placed into an alumina crucible after being mixed in an agate mortar. In order to remove the water, ammonia, and carbon dioxide, the sample was slowly heated to 700 °C in an electrical furnace. Subsequently, the calcination products were melted at the temperature range of 1100–1200 °C, depending on their chemical composition. The resulting melt was poured onto a preheated (300 °C) brass mold and annealed for 2 h at the temperature that was approximately 5 °C below the glass transition temperature (T_g). The values of the glass transition temperature and the thermal expansion coefficient of glass, α_g, taken from the work of Lee and Taylor [31] are summarized in Table 1.

Raman spectra were recorded using RENISHAW inVia Reflex Raman spectrometer with Leica DM2500 microscope. The semiconductor laser (532 nm, 28.5 mW) was used as the excitation source with the spot of about 1 mm diameter. After the baseline subtraction, the spectra were corrected by the Böse–Einstein population factor [32]:

$$I_{cor} = I_{exp} \nu \nu_0^3 \frac{1 - \exp\left[-hc\nu/kT\right]}{\left(\nu_0 - \nu\right)^4} \qquad (1)$$

where I_{exp} and I_{cor} are observed and corrected Raman intensities, ν and ν_0 are the Raman shift and the wavenumber of the excitation laser, and h, k, c, and T represent Planck's constant, Boltzmann's constant, the speed of light, and thermodynamic temperature. Furthermore, all spectra were normalized to the height of the highest peak [33].

Results and discussion

The set of five baseline subtracted and thermally corrected Raman spectra of xBaO·$(1-x)$ P_2O_5 ($x = 0.30$, 0.35, 0.40, 0.45, and 0.50) glasses was analyzed (Fig. 1). The spectra

Table 1 Glass transition temperature T_g [31], thermal expansion coefficient of glass α_g [31], and results of SVTDM with corresponding Q-distribution for studied glasses

x_g(BaO)	T_g/°C	$10^7 \cdot \alpha_g$/°C^{-1}	n(P)/mol	n(BP2)/mol	n(BP)/mol	$n(Q^3)$/mol	$n(Q^2)$/mol
0.30	421	124	0.10	0.30	0.00	0.80	0.60
0.35	437	128	0.00	0.30	0.05	0.60	0.70
0.40	452	131	0.00	0.20	0.20	0.40	0.80
0.45	458	134	0.00	0.10	0.35	0.20	0.90
0.50	478	137	0.00	0.00	0.50	0.00	1.00

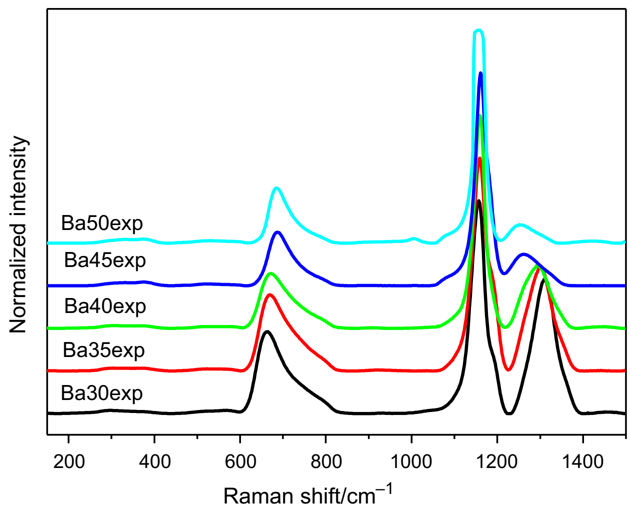

Fig. 1 Normalized and thermally corrected Raman spectra

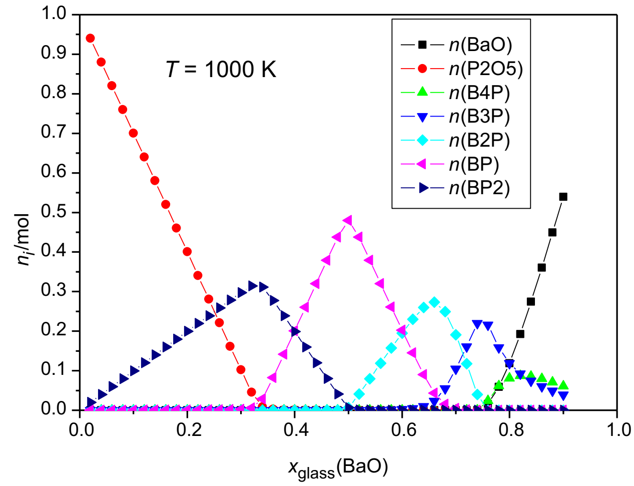

Fig. 3 Thermodynamic model of Shakhmatkin and Vedishcheva (SVTDM)—equilibrium molar amounts of system components at temperature $T = 1000$ K

were recorded with a wavenumber step of 2 cm^{-1} in the range (150–1500) cm^{-1}.

MATLAB software was used for the principal component analysis [27]. The real error of 2.6% approaches the experimental error for two components. The PCA analysis resulted in two independent components. This is because the indicator function [26, 27] had a minimum (Fig. 2), and the Malinowski significance fell to 8%, when using two components.

The SVTDM was evaluated well above T_g at a temperature of 1000 K (Fig. 3). The seven following system components, which are defined as stable crystalline phases of the $BaO–P_2O_5$ binary phase diagram, were considered: BaO, P_2O_5, $4BaO·P_2O_5$ (B4P), $3BaO·P_2O_5$ (B3P), $2BaO·P_2O_5$ (B2P), $BaO·P_2O_5$ (BP), and $BaO·2\ P_2O_5$ (BP2). The FACT database was used to gather the molar Gibbs energies of the components listed above [21]. The thermodynamic model behaves like a quasi-binary system at temperatures above T_g (i.e., maximum two system components can be found with nonzero abundance). Therefore, the mass conservation law can be used to evaluate the equilibrium molar quantities of system components for all studied glass compositions at their T_g. For example, when applied to the xBaO·$(1-x)$ P_2O_5 glass composition we obtain the following relation:

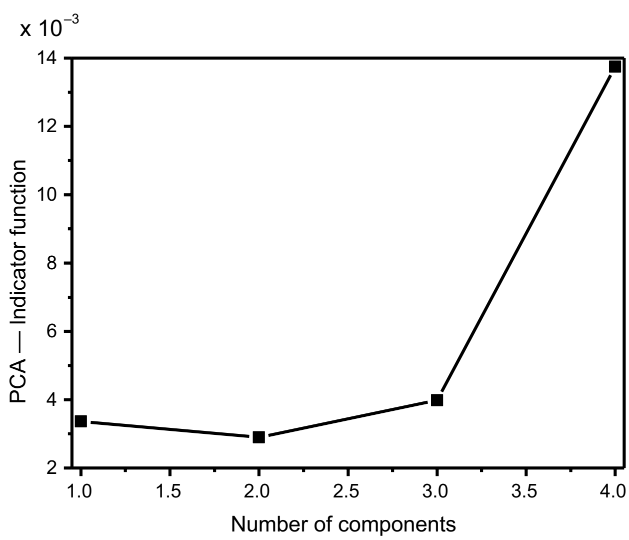

Fig. 2 PCA—indicator function—reaches minimum for two components

– for $0 \leq x \leq 1/3$, only P and BP2 are present with a non-negligible equilibrium molar content, n_i.

$$n(\mathrm{BP2}) = x \tag{2}$$

$$n(\mathrm{P}) = 1 - 3x \tag{3}$$

– for $1/3 \leq x \leq 0.5$, only BP2 is present with non-negligible equilibrium molar content n_i. The mass conservation law gives us:

$$n(\mathrm{BP2}) = 1 - 2x \tag{4}$$

$$n(\mathrm{BP}) = 3x - 1 \tag{5}$$

The resulting equilibrium molar amounts and the corresponding Q-distributions are summarized in Table 1. It is shown that only two Q-units are present in the studied glass compositions. Only two system components (i.e., BP2 and BP) are present in nonzero equilibrium molar amounts for all studied glasses, with the exception of the

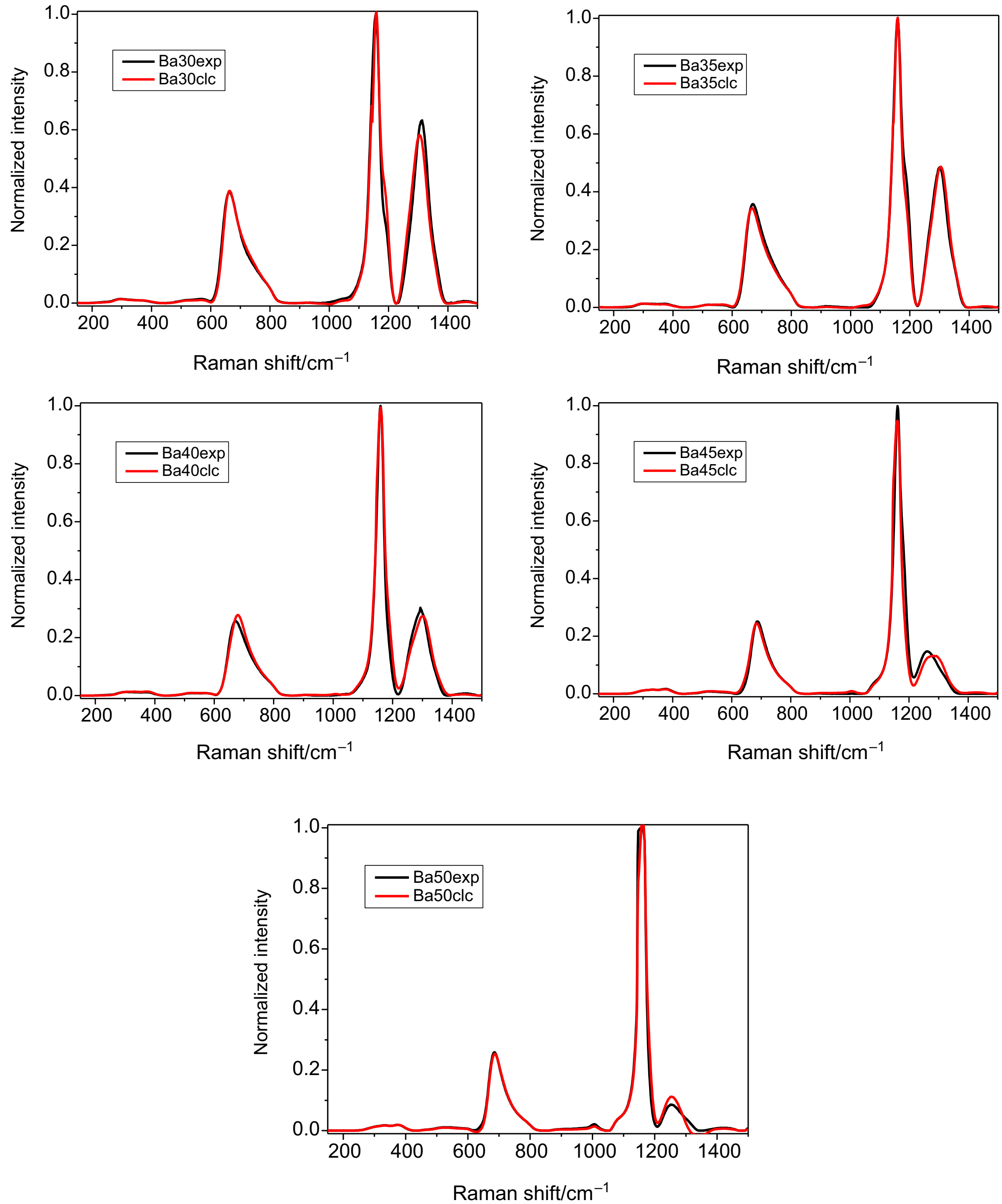

Fig. 4 Comparison of experimental and Malfait's method calculated Raman spectra

x_g(BaO) = 0.3 glass, where a small amount of P_2O_5 was found. This result is in agreement with the result PCA analysis of the experimental Raman spectra. The compositional dependence of Q^2 equilibrium molar amount is similar to the compositional dependence of glass transition temperature and coefficient of thermal expansion α_g (T_g and α_g values were taken from the work of Lee and Taylor [31]). That is, with increase in content of BaO the Q^2 equilibrium molar amount as well as T_g and α_g values increases (Fig. 2).

Therefore, in the next step, Malfait's spectral decomposition was performed with our own FORTRAN program

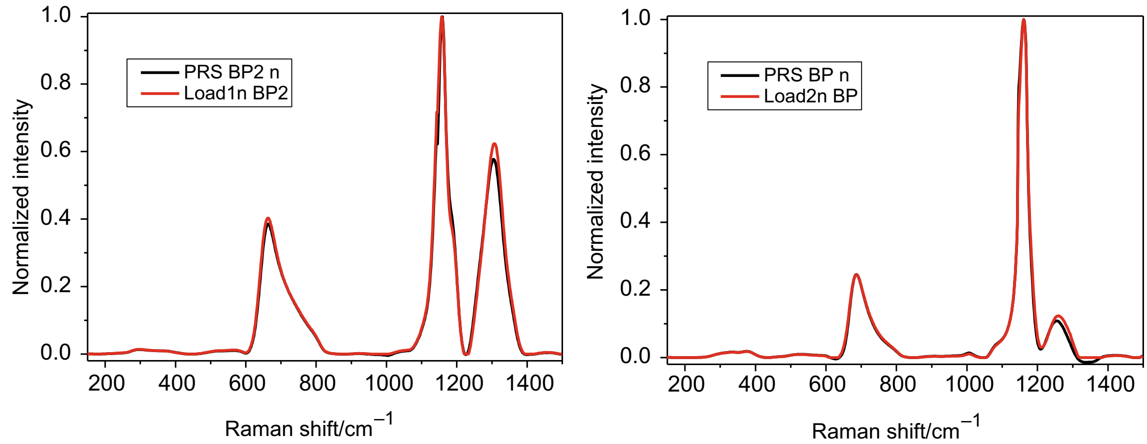

Fig. 5 Comparison of normalized partial Raman spectra BP2 and BP with corresponding normalized MCR loadings

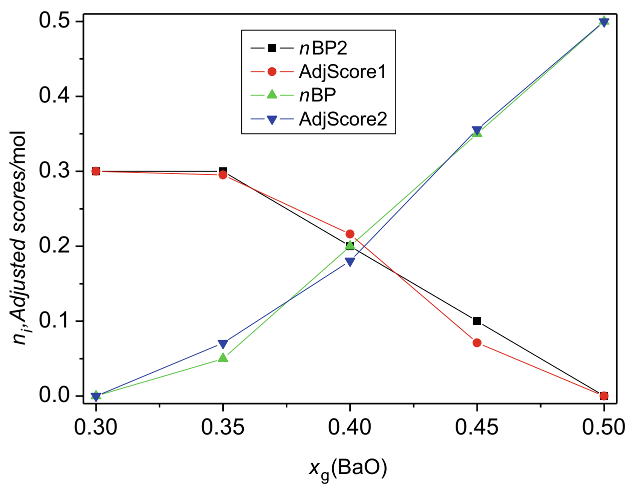

Fig. 6 Comparison of adjusted scores and equilibrium molar amounts of BP and BP2

JaneDove, by using the BP2 and BP equilibrium molar amounts. Such way, two PRS were obtained—the first one corresponding to BP2 with small admixture of P and the second one corresponding to BP. The calculated spectra reproduced the experimental spectra with high accuracy (Fig. 4). The obtained partial Raman spectra of BP2 and BP are plotted in Fig. 5 where they are compared with the corresponding MCR loadings.

MCR [29, 30] performed for two independent components resulted in the Raman spectra (loadings) and relative abundances (scores) of both components (Figs. 4, 5). 98.93% of the spectral data variance was reproduced using the MCR method. Based on the high positive correlation between equilibrium molar amounts and scores, the particular loadings were attributed to the particular system components. In this way, Loading 1 was attributed to BP2, and Loading 2 to BP. It can be seen that normalized MCR loadings are very similar to the normalized PRS (Fig. 5). The MCR results are not unique. All experimental spectra and loadings (i.e., the spectra of "pure" component) can be scaled by multiplying or dividing them by an arbitrary positive constant. Such scaling of the experimental spectra and loadings is shown in the corresponding change of the scores. In this way, scores can be adjusted to reproduce the equilibrium molar amounts of system components. Adjustment of the scores is based on the minimization of the sum of the squares of the differences between scores and their corresponding equilibrium molar amounts. A good agreement between the adjusted scores and equilibrium molar amounts of BP2 and BP system components is illustrated in Fig. 6.

Conclusions

PRS calculated from the SVTDM by the Malfait's method coincide with the loadings calculated by the MCR method. MCR and Malfait's results are based on the results of SVTDM and reproduced the experimental spectra with high accuracy. Such way, the obtained results confirm the SVTDM.

Acknowledgements This paper is created in the frame of the Project FunGlass that has received funding from the European Union's Horizon 2020 research and innovation program under Grant Agreement No. 739566. This work was supported by The Slovak Grant Agency for Science under Grant No. VEGA 1/0064/18, and the Project Centre for Functional and Surface Functionalized Glass (CEGLASS), ITMS code is 313011R453, operational program Research and innovation, co-funded from European Regional Development Fund.

References

1. Černošek Z, Holubová J. The structure and certain properties of $CaO–In_2O_3–P_2O_5$ glasses. J Non-Cryst Solids. 2018;490:44–9.
2. Brow RK. Review: the structure of simple phosphate glasses. J Non-Cryst Solids. 2000;263–264:1–28.
3. Hoppe U. A structural model for phosphate glasses. J Non-Cryst Solids. 1996;195:138–47.
4. Ray NH. Composition–property relationship in inorganic oxide glasses. J Non-Cryst Solids. 1974;15:1423–34.
5. Brow RK, Alam TM, Tallant DR, Kirkpatrick RJ. Spectroscopic studies of phosphate sealing glasses. MRS Bull. 1998;23:63–7.
6. Sales C, Boatner LA. Lead–iron phosphate glass: a stable storage medium for high-level nuclear waste. Science. 1984;226:45–8.
7. Neel EAA, Pickup DM, Valappil SP, Newport RJ, Knowles JC. Bioactive functional materials: a perspective on phosphate-based glasses. J Mater Chem. 2009;19:690–701.
8. Vedishcheva NM, Wright AC. Chemical structure of oxide glasses: a concept for establishing structure–property relationships. In: Schmelzer JWP, editor. GLASS selected properties and crystallization, Chapter 5. Berlin: De Gruyter; 2014, p. 269–99. ISBN 978-3-11-029838-3.
9. Vedishcheva NM, Shakhmatkin BA, Shultz MM, Wright AC. The thermodynamic modelling of glass properties: a practical proposition? J Non-Cryst Solids. 1996;196:239–43.
10. Shakhmatkin BA, Vedishcheva NM, Wright AC. Can thermodynamics relate the properties of melts and glasses to their structure? J Non-Cryst Solids. 2001;293–295:220–36.
11. Vedishcheva NM, Shakhmatkin BA, Wright CA. Thermodynamic modeling of the structure of glasses and melts: single-component, binary and ternary systems. J Non-Cryst Solids. 2001;293–295:312–7.
12. Vedishcheva NM, Shakhmatkin BA, Wright CA. The structure of sodium borosilicate glasses: thermodynamic modeling vs. experiment. J Non-Cryst Solids. 2004;345–346:39–44.
13. Macháček J, Chromčíková M, Liška M. Parameterization and validation of thermochemical models of glass by advanced statistical analysis of spectral data. In: Šesták J, Hubík P, Mareš JJ, editors. Thermal physics and thermal analysis: from macro to micro, highlighting thermodynamics kinetics and nanomaterials, Chapter 12. Switzerland: Springer; 2017, p. 257–78. ISBN 978-3-319-45897-7.
14. Liška M, Chromčíková M. Thermal properties and related structural and thermodynamic studies of oxide glasses. In: Šesták J, Holeček M, Málek J, editors. Glassy, amorphous and nano-crystalline materials: thermal physics, analysis, structure and properties, Chapter 11. New York: Springer; 2011, p. 179–97. ISBN 978-90-481-2882-2.
15. Chromčíková M, Liška M, Karell R, Gašpáreková E, Vlčková P. Thermodynamic model and physical properties of selected zirconia containing silicate glasses. J Therm Anal Calorim. 2012;109:831–40.
16. Chromčíková M, Liška M, Macháček J, Šulcová J. Thermodynamic model and structure of $CaO–P_2O_5$ glasses. J Therm Anal Calorim. 2013;114:785–9.
17. Chromčíkova M, Liška M, Zemanová V, Plško A, Hruška B, Gavenda T. Thermodynamic model and Raman spectra of $CaO–P_2O_5$ glasses. J Therm Anal Calorim. 2015;121:269–74.
18. Liška M, Lissová M, Plško A, Chromčíková M, Gavenda T, Macháček J. Thermodynamic model and Raman spectra of $ZnO–P_2O_5$ glasses. J Therm Anal Calorim. 2015;121:85–91.
19. Hruška B, Osipov AA, Osipova LM, Chromčíková M, Černá A, Liška M. Thermodynamic model and high-temperature Raman spectra of $25Na_2O·75B_2O_3$ glassforming melts. J Therm Anal Calorim. 2018;133:429–33.
20. Voňka P, Leitner J. Calculation of chemical equilibria in heterogeneous multicomponent systems. Calphad. 1995;19:25–36.
21. http://www.crct.polymtl.ca/fact/. Accessed 18 April 2017.
22. Bale CW, Bélisle E, Chartrand P, Decterov SA, Eriksson G, Hack K, Jung IH, Kang Y-B, Melançon J, Pelton AD, Robelin C, Petersen S. FactSage thermochemical software and databases—recent developments. Calphad. 2009;33:295–311.
23. Malfait WJ, Zakaznova-Herzog VP, Halter WE. Quantitative Raman spectroscopy: high-temperature speciation of potassium silicate melts. J Non-Cryst Solids. 2007;353:4029–42.
24. Malfait WJ, Halter WE. Structural relaxation in silicate glasses and melts: results from high-temperature Raman spectroscopy. Phys Rev B. 2008;77:014201.
25. Malfait WJ. Quantitative Raman spectroscopy: speciation of cesium silicate glasses. J Raman Spectrosc. 2009;40:1895–901.
26. Malinowski ER. Factor analysis in chemistry. 3rd ed. New York: Wiley; 2002.
27. Factor analysis toolbox for MATLAB®. www.chemometrics.com (2017). Accessed 22 June 2017.
28. Castro SAD, Virgens CF. Thermal decomposition of Nephelium lappaceum *L. peel*. J Therm Anal Calorim. 2019;137:1–9.
29. Ruckebusch C, Blanchet L. Multivariate curve resolution: a review of advanced and tailored applications and challenges. Anal Chim Acta. 2013;765:28–36.
30. http://www.eigenvector.com/courses/EigenU_MCR.html. Accessed 2 July 2019.
31. Lee ETY, Taylor ERM. Optical and thermal properties of binary calcium phosphate and barium phosphate glasses. Opt Mater. 2006;28:200–6.
32. Osipov AA, Osipova LM. Structural studies of $Na_2O–B_2O_3$ glasses and melts using high-temperature Raman spectroscopy. Phys B. 2010;405:4718–32.
33. Kalenda P, Koudelka L, Mošner P, Beneš L, Drobná H. Thermoanalytical study and crystallization of $Ba(PO_3)_2–WO_3$ glasses. J Therm Anal Calorim. 2019. https://doi.org/10.1007/s10973-019-08115-w.